Accepted Manuscript

Novel pyrazole-5-carboxamide and pyrazole-pyrimidine derivatives: synthesis and anticancer activity

Jing Bo Shi , Wen Jian Tang , Xing Bao qi , Jun Li , Rong Li , Xin Hua Liu

PII: S0223-5234(14)01122-2

DOI: 10.1016/j.ejmech.2014.12.013

Reference: EJMECH 7573

To appear in: *European Journal of Medicinal Chemistry*

Received Date: 5 September 2014

Revised Date: 4 December 2014

Accepted Date: 8 December 2014

Please cite this article as: J.B. Shi, W.J. Tang, X. Bao qi, J. Li, R. Li, X.H. Liu, Novel pyrazole-5-carboxamide and pyrazole-pyrimidine derivatives: synthesis and anticancer activity, *European Journal of Medicinal Chemistry* (2015), doi: 10.1016/j.ejmech.2014.12.013.

Graphical abstract

Novel pyrazole-5-carboxamide and pyrazole-pyrimidine derivatives: synthesis and anticancer activity

Jing Bo Shi[a,*], Wen Jian Tang [a], Xing Bao qi[a], Jun Li [a], Rong Li [a], Xin Hua Liu [a,b*]

[a] *School of Pharmacy, Anhui Medical University, Hefei, 230032, P. R. China*

[b] *State Key Laboratory of Pharmaceutical Biotechnology, Nanjing University, Nanjing 210093, P. R. China*

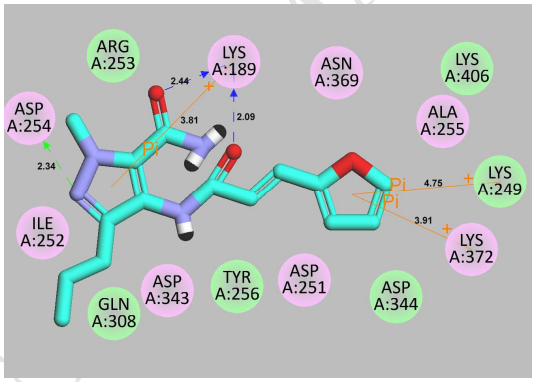

Novel pyrazole-5-carboxamide and pyrazolo[4,3-d]pyrimidine derivatives were designed and synthesized. Compound **8e** exhibited strong inhibitory activity against MGC-803 cells, and showed the most potent telomerase inhibitory activity.

Novel pyrazole-5-carboxamide and pyrazole-pyrimidine derivatives: synthesis and anticancer activity

Jing Bo Shi[a,*], Wen Jian Tang [a], Xing Bao qi[a], Jun Li [a], Rong Li [a], Xin Hua Liu [a,b*]

[a] *School of Pharmacy, Anhui Medical University, Hefei, 230032, P. R. China*

[b] *State Key Laboratory of Pharmaceutical Biotechnology, Nanjing University, Nanjing 210093, P. R. China*

Abstract: A series of novel pyrazole-5-carboxamide and pyrazole-pyrimidine derivatives were designed and synthesized. All compounds have been screened for their antiproliferative activity against MGC-803, SGC-7901 and Bcap-37 cell lines *in vitro*. The results revealed that compounds **8a**, **8c** and **8e** exhibited strong inhibitory activity against MGC-803 cell line. The flow cytometric analysis result showed that compound **8e** could inhibit MGC-803 proliferation. Some title compounds were tested against telomerase, and compound **8e** showed the most potent inhibitory activity with IC_{50} value at 1.02±0.08 μM. The docking simulation of compound **8e** was performed to get the probable binding model, among them, LYS 189, LYS 372, LYS 249 and ASP 254 may be the key residues for the telomerase activity.

Keywords: Synthesis; pyrazole-5-carboxamide; anticancer activity; telomerase

*Corresponding author.

Tel.: +86 551 65161115; fax: +86 551 65161115. E-mail: sjb0616@126.com.

+86 551 65161115; fax: +86 551 65161115. E-mail: xhliuhx@163.com.

1. Introduction

Telomerase is active in the early stages of life. In majority of adult somatic cells, it turns to dormancy. However, in cancer cells, telomerase is reactivated to keep the telomere length short in rapidly dividing cells, leading to proliferation. So, telomerase represents one of the promising targets in drug discovery [1-4]. Telomere and telomerase closely related to the occurrence and development of gastric cancer has been reported [5]. In recent publications, one new hypothesis could be utilized to explain the association between telomerase TERT (human telomerase reverse transcriptase) and cancers. The regulation of telomerase TERT predominantly leads to cell proliferation or apoptosis, ultimately resulting in anticancer activity. Unfortunately, these broad-spectrum telomerase TERT inhibitors have been limited by non-specificity and thus non-selective toxicity and dose-limiting efficacy. Therefore, the pursuit of novel telomerase inhibitors with better antitumor effects and more safety profile is still the main issue. ·

The pyrazole-pyrimidine and their bioisosteres are heterocyclic compounds with important biological functions including antitumor and other activities [6-8]. As is known to all that pyrazole-pyrimidine derivatives PP242, PP30 and PDE5 (Figure 1) have possessed good kinase selectivity profile used as cyclin-dependent kinase (CDK), ATP-competitive mTORC1/mTORC2 inhibitors [9-16]. It was of our interest to utilize rational chemical approaches to generate and identify novel compounds as potential telomerase inhibitors for cancer therapy. Results of structure-activity relationships (SAR) about these derivatives show that the alkyl of the position 1 or 3 should help the activity, there is some motivations provided in the design idea [17-20]. Furthermore, based on the protein TERT structure of telomerase using LigandFit module, our group has recently reported a novel docking model and we found that ASP 254 was a key residue for activity. Focusing on residue ASP 254 and the volume of the active site of hTERT, we therefore designed some of synthesizable drug-like scaffolds which incorporate the moiety of pyrazole-pyrimidine.

In our recent works [21,22], several pyrazole derivatives were designed, which had potent anticancer activity as potential telomerase inhibitors. Because moiety

pyrazole-5-carboxamide is a precursor of title pyrazole-pyrimidine structure (Figure 2), in order to summarize the SAR, we have also carried out active screening against them. In this study, a series of novel small molecules elaborated around pyrazole-5-carboxamide and pyrazole-pyrimidine scaffolds were designed. We also will built the relative SAR between pyrazole-pyrimidines to their precursors as antitumor agents, which maybe rationalize the experimental observations and guide us to screen good potency telomerase inhibitors in the further study.

(Figures 1-2)

2. Results and discussion

2.1 Chemistry

All derivatives were synthesized by acylation reaction starting from 1-methyl-4-nitro-3-*N*-propylpyrazole-5-carboxamides **7**, which was prepared from 2-pentanone via claisen condensation, hydrazinolytic, cyclization, methylation, hydrolysis, nitration, amidation, reduction according to Scheme 1. Compounds **8a-e** were obtained through two steps: First, the substituted carboxylic acids were converted into acyl chlorides with oxalyl chloride at room temperature and excess oxalyl chloride was evaporated, then the acyl chloride was directly reacted with compounds **7** to form amide compounds **8a-e**. Compounds **9a-e** were obtained from compounds **8a-e** via cyclization. The reaction was carried out in the presence of sodium ethoxide, the EtOH used as solvent at reflux condition. All compounds were characterized by means of HR-MS, ^{1}H NMR and ^{13}C NMR spectral analysis.

(Scheme 1)

2.2 Crystal structure analysis

The structures of compounds **8d** and **9a** were determined by X-ray crystallography. Crystal data of **8d**: Colorless crystals, yield, 77%; mp 151-152 ^{o}C; $C_{18}H_{24}N_4O_5$, Monoclinic, space group P_12_1/c; a = 14.4205(14), b = 17.7873(16), c = 8.8377(9) (Å); α =

90, β = 100.983(10), γ= 90 (°), V = 2225.4(4) nm^3, T =293(2) K, Z =4, Dc = 1.261 g/cm^3, $F(000)$= 904, Reflections collected / unique = 9519 / 4373, Data / restraints / parameters = 4373 / 6 / 279, Goodness of fit on F^2 =1.087, Fine, R_1= 0.0681, $wR(F^2)$ = 0.1722. Crystal data of **9a**: Colorless crystals, yield, 85%; mp 200-201^{o}C; $C_{17}H_{18}N_4O$, Monoclinic, space group P_12_1/c; a = 16.820(5), b = 5.381(3), c = 18.370(6) (Å); α = 90, β = 112.73(4), γ= 90 (°), V = 1533.4(11) nm^3, T =293(2) K, Z =4, Dc = 1.275 g/cm^3, $F(000)$= 624, Reflections collected / unique = 3274/ 1312, Data / restraints / parameters = 3274 / 0 / 202, Goodness of fit on F^2 =0.880, Fine, R_1= 0.0741, $wR(F^2)$ = 0.1818. Their molecular structures were shown in Figure 3. Crystallographic data (excluding structure factors) for the structures had been deposited with the Cambridge Crystallographic Data Center as supplementary publication No. CCDC-981021 and 1021035.

(Figure 3)

2.3 In vitro anticancer activity

Recently, we focused on screening lead compounds with specific activity against gastric cancer cells, so gastric cancer cell SGC-7901 and MGC-803 were chosen. In this screening assay studies, all the compounds were evaluated for their cytotoxic activity against SGC-7901, MGC-803 cell lines. In order to examine activity with other cancer cells, Bcap-37 (human breast cancer cell line) was chosen. The results were reported in terms of IC_{50} values (Table 1).

In the initial study of SAR, our title compounds were divided into two series, one was the 5-propyl-1H-pyrazole-3-carboxamide (compounds **8a~8e**), the other was the pyrazolo[4,3-d]pyrimidin-7(6H)-one (compounds **9a~9e**). Among them, compound **8** is the precursor of compound **9**. In general, series 5-propyl-1H-pyrazole-3-carboxamide (compounds **8**) leded to increase in inhibitory activity, among them, compound **8a** was the most potent activity against MGC-803 cell with IC_{50} value of 3.01±0.23 μM, surpassing that of the positive control 5-fluorouracil. Compared with the compounds **8**, compounds **9** generally did not reflect the activity on the tested cells (**9b, 9d**). Therefore, for this kind of

structure moiety, activity of precursor compounds was superior to that cyclization compounds.

The SAR also indicated that all title compounds showed good activity against gastric cancer cells but poor activity against Bcap-37 cells. Scanning from Table 1, it is obvious that compounds **8a, 8b** and **8c** exhibited the strong inhibitory activity against the MGC-803 cells (with IC_{50s} of 3.44±0.28, 4.57±0.88, 4.24±1.22 μM, respectively) and the values could compare with that of the potent 5-fluorouracil.

(Table 1)

2.4 Cell Cycle Analysis

To understand whether the cell cycle arrest lead to decrease cell proliferation [23], we used flow cytometric analysis to measure the effect of compound **8e** on induction of cell cycle. As shown in Figure 4, the cells in S phase in the MGC-803 control group accounted for about 30.38%, while after cells treated with compound **8e** MGC-803 for 48 h, the ratio was approximately 42.16%. This showed that the cells were arrested in S phase.

(Figure 4)

2.5 Telomerase activity

Some compounds were assayed for telomerase inhibition, using MGC-803 cells extract, ethidium bromide and BIBR1532 were used as the reference compounds. The results (Table 2) suggested that compounds **8a** and **8e** showed strong telomerase inhibitory activity with IC_{50} values of 1.98±0.21, 1.02±0.08 μM respectively, which surpassing that of the positive control ethidium bromide, comparable to that of positive control BIBR1532, furthermore, there was a good correlation between antiproliferative activity and telomerase activity of compound **8e** (Tables 1 and 2). Among them, compound **8e** *(E)*-4-(3-(furan-2-yl)acrylamido)-1-methyl-3-propyl-1H-pyrazole-5-carboxamide showed higher inhibitory activity than the others. This also pointed out the direction for us to

further optimize the structure of 1H-pyrazole-5-carboxamide moiety with anticancer activity as potential telomerase inhibitors.

(Table 2)

2.6 Molecular docking

In an effort to elucidate the mechanism by which the title compound exhibited strong inhibitory activity against telomerase and to establish SAR based on our experimental studies, molecule docking of the compound **8e** into active site containing key residue ASP 254 was performed to simulate a binding model derived from telomerase TERT (3DU6. pdb). In general, compound **8e** could fit well into the catalytic subunit of telomerase (TERT) and inhibit telomerase activity as a substitute of substrate nucleotides. There are six obvious interactions diagram were shown. The binding model of compound **8e** with TERT was depicted in Figure 5. The 2D and 3D pictures of binding were depicted in Figure 5A and Figure 5B. In order to reveal that the molecule was well filled in the active pocket, the enzyme surface was shown in Figure 5C. There are six obvious bonding interactions anchoring compound **8e** to the active site tightly might explain its good inhibitory activity. First, we found hydrogen bond between the backbone amino groups of ASP 254 and **N** atom of pyrazole moiety. Another two hydrogen bonds interaction were between the LYS 189 and the **O** atoms of amide. Second, three Pi-Cation interactions were formed (pyrazole ring with LYS 189; furan ring with the LYS 372 and LYS 249, respectively).

(Figure 5)

3. Conclusions

In brief, based on rational design and reasonable analysis, we designed some novel 1H-pyrazole-5-carboxamide derivatives. Next, these compounds used as precursors due to exploring reasonable SAR, some new 1H-pyrazolo[4,3-d]pyrimidin-7(6H) derivatives were designed, followed by chemical synthesis and biological evaluated for them. The

results revealed that some 1H-pyrazole-5-carboxamide compounds reflected high activity against gastric cancer cells. Among them, compound **8e** exhibited strong inhibitory activity against MGC-803 cells, and showed the most potent telomerase inhibitory activity with IC_{50} value at 1.02±0.08 μM. Flow cytometric analysis indicated that the cells were arrested in S phase by compound **8e**. The docking simulation was performed to get the probable binding models poses and the key residues ASP 254, LYS 189, LYS 372, LYS 249. Compared with our previous work, the advantage of this study was that new skeleton structure targeting telomerase was found. These results are of help in the rational design of higher selectivity telomerase inhibitors in further.

4. Experimental section

4.1 Chemistry

The reactions were monitored by thin layer chromatography (TLC) on pre-coated silica GF254 plates. Melting points were determined on a XT4MP apparatus (Taike Corp., Beijing, China), and are uncorrected. ^{1}H and ^{13}C NMR spectra were recorded on a Brucker AM-300 (300 MHz) spectrometer with $CDCl_3$ or DMSO-d_6 as the solvent and TMS as the internal standard. Chemical shifts are reported in δ (parts per million) values. Coupling constants *J* are reported in Hz. High-resolution electron impact mass spectra (HR-MS) were recorded under electron impact (70 eV) condition using a MicroMass GCT CA 055 instrument. All chemicals or reagents were purchased from standard commercial suppliers and treated with standard methods before use. Solvents were dried in a routine way and redistilled.

*4.2. General procedure for the synthesis of title compounds **8***

To a methylene chloride (10mL) solution of substituted Carboxylic acid 3 (5 mmol) in an ice bath was added oxalyl chloride (10 mmol), and catalytic *N*,*N*-Dimethylformamide, while the reaction contents were stirred continuously. The reaction mixture was allowed to stand at 25-30 ^{o}C for 3 h. Solvent distilled under reduced pressure and dried under high vacuum to remove oxalyl chloride. Reaction mass was dissolved in dichloromethane (10 ml). The solution was added to the mixture of amine 7 (4.5 mmol) and TEA (10 mmol) and then allowed to stir at room temperature for overnight. Reaction mixture was washed with

saturated sodium bicarbonate (20 ml) and then with water (20 ml). Organic solvent was dried over anhydrous Na_2SO_4, filtrated, and then evaporated to give solid. Crude solid product was recrystallied from suitable solvent to give title compounds **8a-e** (Scheme 1) as solids.

8a: *4-cinnamamido-1-methyl-3-propyl-1H-pyrazole-5-carboxamide*

Off-white powder solid, yeild, 75%; mp: 225-226 ^oC (recryst. from ethanol); ^1H NMR (300 MHz, $CDCl_3$+DMSO-d_6) δ (ppm): 9.03 (Brs, 1H, NH), 7.56 (d, *J*=15.52, 1H, Ar-CH), 7.36 (s, 2H, ArH), 7.21 (m, 3H, ArH), 6.54 (d, *J*=15.72, 1H, CO-CH), 6.13 (Brs, 2H, NH_2), 3.86 (s, 3H, N-CH_3), 2.35 (t, *J* = 7.6 Hz 2H, N-CH_2), 1.45 (m, 2H, CH_2), 0.78 (t, *J* = 7.0 Hz, 3H, CH_3). HR-MS: calcd for $C_{17}H_{20}N_4O_2$ $[M+Na]^+$, 335.1478; found 335.1479.

8b: *1-methyl-3-propyl-4-(3,4,5-trimethoxybenzamido)-1H-pyrazole-5-carboxamide*

Off-white powder solid, yeild, 73%; mp: 190-191 ^oC (recryst. from ethanol); ^1H NMR (300 MHz, $CDCl_3$) δ (ppm): 7.98+7.74 (Brs, 1H, NH), 7.12 (d, 2H, ArH), 5.69 (Brs, 2H, NH_2), 3.92 (s, 12H, 3O-CH_3, N-CH_3), 2.53 (m, 2H, N-CH_2), 1.63 (m, 2H, CH_2), 0.92 (m, 3H, CH_3). HR-MS: calcd for $C_{18}H_{24}N_4O_5$ $[M+Na]^+$, 399.1639; found 399.1638.

8c: *(E)-1-methyl-3-propyl-4-(3-(3,4,5-trimethoxyphenyl)acrylamido)-1H-pyrazole-5-carboxamide*

Off-whit powder solid, yeild, 80%; mp: 203-204 ^oC (recryst. from ethanol); ^{1}HNMR (300 MHz, $CDCl_3$+DMSO-d_6) δ (ppm): 9.62 (Brs, 1H, NH), 7.62 (d, J=15.63, 1H, Ar-CH), 6.81 (s, 2H, ArH), 6.69 (d, J=15.63, 1H, CO-CH), 4.14 (s, 3H, N-CH_3), 3.90 (s, 6H, 2 O-CH_3), 3.85 (s, 3H, O-CH_3), 2.51 (t, *J* = 7.6 Hz, 2H, N-CH_2), 1.62 (m, 2H, CH_2), 0.91 (t, *J* = 7.3 Hz, 3H, CH_3). HR-MS: calcd for $C_{20}H_{26}N_4O_5$ $[M+Na]^+$, 425.1795; found 425.1794.

8d: *1-methyl-3-propyl-4-(2,4,5-trimethoxybenzamido)-1H-pyrazole-5-carboxamide*

Off-whit powder solid, yeild, 77%; mp: 150-151 ^oC (recryst. from ethanol); ^1H NMR (300 MHz, $CDCl_3$) δ (ppm): 9.30 (Brs, 1H, NH), 8.0+5.60 (Brs, 2H, NH_2), 7.83 (s, 1H, ArH), 6.60 (s, 1H, ArH), 4.08 (s, 3H, N-CH_3), 3.93~4.05 (s, 9H, 3O-CH_3), 2.61(t, *J* = 7.5 Hz, 2H, N-CH_2), 1.63 (m, 2H, CH_2), 0.94 (t, *J* = 7.3 Hz, 3H, CH_3). HR-MS: calcd for $C_{18}H_{25}N_4O_5$ $[M+H]^+$, 377.1819, found 377.1824.

8e: *(E)-4-(3-(furan-2-yl)acrylamido)-1-methyl-3-propyl-1H-pyrazole-5-carboxamide*

Light brown powder solid, yeild, 65%; mp: 249-252 ^oC (recryst. from 95% ethanol);

^{1}H NMR (300 MHz, DMSO-d_6) δ (ppm): δ 9.57 (Brs, 1H, NH), 7.83 (d, J = 1.3 Hz, 1H, Furan-H), 7.73 (s, 1H, Furan-H), 7.41 (d, J = 15.6 Hz, 1H, Ar-CH), 6.86 (d, J = 3.4 Hz, 1H, Furan-H), 6.63 (d, J = 15.6 Hz, 1H, CO-CH), 3.88 (s, 3H, N-CH_3), 2.37 (t, *J* = 7.5 Hz, 2H, N-CH_2), 1.59-1.46 (m, 2H, CH_2), 0.86 (t, J = 7.4 Hz, 3H, CH_3).

4.3. General procedure for the synthesis of title compounds ***9***

Compound **8** (1 mmol) and sodium ethoxide (5 mol) were dissolved in ethanol (15 mL), and refluxed for 12 h. After completion of the reaction, the solvent was concentrated to a low volume; the residue was added HCl (1N), the precipitated product was granulated at pH 7 and 10 ^{o}C for a further hour. The title compounds **9a-9e** was collected by filtration, washed with water, and dried to give as solid.

9a: *(E)-1-methyl-3-propyl-5-styryl-1H-pyrazolo[4,3-d]pyrimidin-7(6H)-one*

Off-whit powder solid, yeild, 85%; mp: 200-201^{o}C; ^{1}H NMR (300 MHz, $CDCl_3$) δ (ppm): 11.60 (Brs, 1H, NH), 7.80 (d, J=16.5, 1H, Ar-CH), 7.60 (d, *J* = 7.1 Hz, 2H, ArH), 7.39(m, *J* = 6.8 Hz, 3H, ArH), 6.96 (d, J=16.5, 1H, CO-CH), 4.28(s, 3H, N-CH_3), 2.92 (t, *J* = 7.5 Hz, 2H, N-CH_2), 1.84 (m, 2H, CH_2), 1.03 (t, *J* = 7.3 Hz, 3H, CH_3). ^{13}CNMR (75 MHz, $CDCl_3$): 156.27, 149.17, 146.78, 139.63, 136.99, 135.57, 129.65, 129.07, 127.54, 124.35, 121.54, 38.34, 27.85, 22.56, 14.24.

9b: *1-methyl-3-propyl-5-(3,4,5-trimethoxyphenyl)-1H-pyrazolo[4,3-d]pyrimidin-7(6H) -one*

Off-whit powder solid, yeild, 84%; mp: 204-206 ^{o}C; ^{1}H NMR (300 MHz, $CDCl_3$) δ (ppm): δ 11.05 (Brs, 1H, NH), 7.29 (s, 2H, ArH), 4.24 (s, 3H, N-CH_3), 4.00 (s, 6H, 2 x O-CH_3), 3.88 (s, 3H, O-CH_3), 2.95 (t, *J* = 7.6 Hz, 2H, N-CH_2), 1.95–1.78 (m, 2H, CH_2), 1.04 (t, *J* = 7.3 Hz, 3H, CH_3).

9c: *(E)-1-methyl-3-propyl-5-(3,4,5-trimethoxystyryl)-1H-pyrazolo[4,3-d]pyrimidin-7 (6H)-one*

Off-whit powder solid, yeild, 81%; mp: 266-270 ^{o}C; ^{1}H NMR (300 MHz, $CDCl_3$) δ (ppm): δ 11.61 (Brs, 1H, NH), 7.67 (d, J = 16.4 Hz, 1H, Ar-CH), 6.91 (d, J = 16.4 Hz, 1H, CO-CH), 6.82 (s, 2H, ArH), 4.29 (s, 3H, N-CH_3), 3.91 (d, 9H, 3O-CH_3), 2.92 (t, *J* = 7.6 Hz, 2H, N-CH_2), 1.93 – 1.77 (m, 2H, CH_2), 1.04 (t, J = 7.3 Hz, 3H, CH_3). HR-MS: calcd for $C_{20}H_{25}N_4O_4$ $[M+H]^+$, 385.187; found 385.1874.

9d: *1-methyl-3-propyl-5-(2,4,5-trimethoxyphenyl)-1H-pyrazolo[4,3-d]pyrimidin-7 (6H)-one*

Off-whit powder solid, yeild, 82%; mp: 184-187 ^{o}C; ^{1}H NMR (300 MHz, $CDCl_3$) δ (ppm): δ 10.99 (Brs, 1H, NH), 8.04 (s, 1H, ArH), 6.59 (s, 1H, ArH), 4.27 (s, 3H, N-CH_3), 4.05 (s, 3H, O-CH_3), 3.98 (s, 6H, 2O-CH_3), 2.94 (t, *J*=7.71, 2H, N-CH_2), 1.95–1.81 (m, 2H, CH_2), 1.04 (t, *J* = 7.4 Hz, 3H, CH_3). HR-MS: calcd for $C_{18}H_{23}N_4O_4$ $[M+H]^+$, 359.1716; found 359.1716.

9e: *(E)-5-(2-(furan-2-yl)vinyl)-1-methyl-3-propyl-1H-pyrazolo[4,3-d]pyrimidin-7(6H)-one*

Light brown powder solid, yeild, 79%; mp: 270-272 ^{o}C; ^{1}H NMR (300 MHz, DMSO-d_6) δ (ppm): δ 12.29 (Brs, 1H, NH), 7.82 (d, *J* = 1.5 Hz, 1H, Ar-CH), 7.64 (d, *J* = 15.84 Hz, 1H, CO-CH), 6.85 (d, *J* = 3.3 Hz, 1H, Furan-H), 6.80 (d, *J* = 15.84 Hz , 1H, Furan-H), 6.63 (dd, *J* = 3.4, 1.8 Hz, 1H, Furan-H), 4.12 (s, 3H, N-CH_3), 2.77 (t, *J* = 7.5 Hz, 2H, N-CH_2), 1.81–1.69 (m, 2H, CH_2), 0.95 (t, *J* = 7.4 Hz, 3H, CH_3).

4.4 Crystallographic Studies

A colorless single crystal of title compounds **8d** and **9a** were chosen for X-ray diffraction analysis performed on a BRUCKER SMART APEX-CCD diffractometer equipped with a graphite monochromatic MoKa radiation (λ = 0.71073 A) radiation at 296(2) K. A total reflections were collected in the range of 2.30<θ<25.30^{o} by using a ψ-ω scan mode with independent ones, of which I >2σ(I) were observed and used in the succeeding refinements. The data set was corrected by SADABS program; the structure were solved by direct methods with SHELXS-97 and refined by full-matrix least-squares method on F^2 with SHELXL-97 [24]. The non-hydrogen atoms were refined anisotropically, and the hydrogen atoms were added according to theoretical models. The structures were refined by full-matrix least-squares method on F^2 with SHELXT-97.

4.5 Anticancer assay

The cytotoxicity evaluation was conducted by using a modified procedure as described in the literature. Briefly, target tumor cells were grown to log phase in *RPMI 1640* medium supplemented with 10% fetal bovine serum. After diluting to 3×10^4 cells mL^{-1} with the complete medium, 100 μL of the obtained cell suspension was added to each well of 96-well culture plates. The subsequent incubation was performed at 37 ˚C, 5% CO_2

atmosphere for 24 h before subjecting to cytotoxicity assessment. Tested samples at pre-set concentrations were added to 6 wells with 5-fluorouracil co-assayed as a positive reference. After 48 h exposure period, 25 μL of PBS containing 2.5 mg mL^{-1} of MTT (3-(4, 5-dimethylthiazol-2-yl)-2, 5-diphenyltetrazolium bromide) was added to each well. After 4h, the medium was replaced by 150 μL DMSO to dissolve the purple formazan crystals produced. The absorbance at 570 nm of each well was measured on an ELISA plate reader. The data represented the mean of three experiments in triplicate and were expressed as means ±SD using *Student t* test. The IC_{50} value was defined as the concentration at which 50% of the cells could survive.

4.6 Cell cycle analysis

For cell cycle analysis, we performed cell cycle kit (Beyotime, China). MGC-803 cells were washed three times by cold PBS, and then cells were fixed in 70% ethanol at -20 ˚C for 12 h. After fixation, cells were washed with cold PBS and stained with 0.5 mL of propidium iodide (PI) staining buffer, which contain 200 mg/mL RNase A, 50 μg/mL PI, at 37 ˚C for 30 min in the dark. Analyses were performed on FACScan flow cytometer. The experiments were repeated three times.

4.7 Telomerase activity assay

Compounds were tested in a search for small molecule inhibitors of telomerase activity by using the TRAP-PCR-ELISA assay. In detail, the MGC-803 cells were firstly maintained in DMEM medium (GIBCO, New York, USA) supplemented with 10% fetal bovineserum (GIBCO, NewYork, USA), streptomycin (0.1 mg/mL) and penicillin (100 IU/mL) at 37 °C in a humidified atmosphere containing 5% CO_2. After trypsinization, 5×10^4 cultured cells in logarithmic growth were seeded into T25 flasks (Corning, New York, USA) and cultured to allow to adherence. The cells were then incubated with Staurosporine (Santa Cruz, Santa Cruz, USA) and the drugs with a series of concentration as 60, 20, 6.67, 2.22, 0.74, 0.25 and 0.082l g/mL, respectively. After 24 h treatment, the cells were harvested by cell scraper orderly following by washed once with PBS. The cells were lysed in 150 μL RIPA cell lysis buffer (Santa Cruz, Santa Cruz, USA), and incubated on ice for 30 min. The cellular supernatants were obtained via centrifugation at 12,000 g for 20 min at 4 °C and stored at -80 °C. The TRAP-PCR-ELISA assay was performed

using a telomerase detection kit (Roche, Basel, Switzerland) according to the manufacturer's protocol. In brief, 2 μL of cell extracts were mixed with 48 μL TRAP reaction mixtures. PCR was then initiated at 94 °C, 120 s for predenaturation and performed using 35 cycles each consisting of 94 °C for 30 s, 50 °C for 30 s, 72 °C for 90 s. Then 20 μL of PCR products were hybridized to a digoxigenin (DIG)-labeled telomeric repeat specific detection probe. And the PCR products were immobilized *via* the biotin-labeled primer to a streptavidin-coated microtiter plate subsequently. The immobilized DNA fragment were detected with a peroxidase-conjugated anti-DIG antibody and visualized following addition of the stop regent. The microtitre plate was assessed on TECAN Infinite M200 microplate reader (Mannedorf, Switzerland) at a wavelength of 490 nm, and the final value were presented as mean ±SD.

4.8 General procedure for molecular docking

Discovery Studio 3.1 (DS 3.1, Accelrys Software Inc., San Diego, California, USA). Crystal structure of telomerase (PDB entry 3DU6) was used as template. Hydrogen atoms were added to protein model. The added hydrogen atoms were minimized to have stable energy conformation and to also relax the conformation from close contacts. The active site was defined and sphere of 5 Å was generated around the active site pocket, with the active site pocket of BSAI model using C-DOCKER, a molecular dynamics (MD) simulated-annealingbased algorithm module from DS 3.1. Random substrate conformations are generated using high-temperature MD. Candidate poses are then created using random rigid-body rotations followed by simulated annealing. The structure of protein, substrate were subjected to energy minimization using CHARMm forcefield as implemented in DS 3.1. A full potential final minimization was then used to refine the substrate poses. Based on C-DOCKER, energy docked conformation of the substrate was retrieved for postdocking analysis.

Acknowledgments

The authors wish to thank the National Natural Science Foundation of China (No. 21272008), Anhui Provincial Natural Science Foundation, (1308085MH137), Science and Technological Fund of Anhui Province for Outstanding Youth (1408085J04).

Supporting information

CCDC-981021 (compound **8d**) and CCDC-1021035 (compound **9a**) contain the supplementary crystallographic data for this paper. These data can be obtained free of charge via the URL http:// www.ccdc.cam.ac.uk/conts/retrieving.html (or from the CCDC, 12 Union Road, Cambridge CB2 1EZ, UK; fax: (+44) 1223 336033; e-mail: deposit@ccdc.cam.ac.uk).

References and notes

[1] D. R. Corey, Chem Biol. 16 (2009), 1219-1223.

[2] Z. Ding, C. J. Wu, M. Jaskelioff, E. Ivanova, M. Kost-Alimova, A. Protopopov, G. C. Chu, G. Wang, X. Lu, E. S. Labrot, J. Hu, W. Wang, Y. Xiao, H. Zhang, J. Zhang, B. Gan, S. R. Perry, S. Jiang, L. Li, J. W. Horner, Y. A. Wang, L. Chin, R. A. DePinho, Cell. 148 (2012), 896-907.

[3] J. W. Shay, W. E. Wright, Nat Rev Drug Discov. 5 (2006), 577-584.

[4] S. A. Stewart, A. A. Bertuch, Cancer Res. 70 (2010), 7365-7371.

[5] A. J. Gillis, A. P. Schuller and E. Skordalakes, Nature, 2008, 455, 633–637.

[6] M. Chauhan, R. Kumar, Bioorg. Med. Chem. Lett. 21 (2013) 5657-5668.

[7] Y. L. Li, J. M. Fevig, J. Cacciola, J. Buriak, K. A. Rossi Jr., J. Jona, R. M. Knabb, J. M. Luettgen, P. C. Wong, S. A. Bai, R. R. Wexler, P. Y. S. Lam, Bioorg. Med. Chem. Lett. 16 (2006) 5176-5182.

[8] V. N. Devegowda, J. H. Kim, K. C. Han, E. G. Yang, H. Choo, A. N. Pae, G. Nama, K. I. Choi, Bioorg. Med. Chem. Lett. 20 (2010) 1630-1633.

[9] D. Geffken, R. Soliman, F. S. G. Soliman, M. M. Abdel-Khalek, D. A. E. Issa, Med. Chem. Res. 20 (2011) 408-420.

[10] M. E. Feldman, B. Apsel, A. Uotila, R. Loewith, Z. A. Knight, D. Ruggero, K. M. Shokat, Plos Bio. 7 (2009) e38.

[11] M. R. Janes, J .J. Limon, L. So, J. Chen, R. J. Lim, M. A. Chavez, C. Vu, M. B. Lilly, S. Mallya, S. T. Ong, M. Konopleva, M. B. Martin, P. Ren, Y. Liu, C. Rommel, D. A. Fruman, Nat. Med. 16 (2010) 205-213.

[12] J. A. Menendez, L. Vellon, C. Oliveras-Ferraros, S. Cufí, A. Vazquez-Martin,

Cell Cycle. 10 (2011) 3658-3677.

[13] D. J. Richard, J. C. Verheijen, K. Curran, J. Kaplan, L. Toral-Barza, I. Hollander, J. Lucas, K. Yu, A. Zask, Bioorg. Med. Chem. Lett. 19 (2009) 6830-6835.

[14] A. Zask, J. C. Verheijen, K. Curran, J. Kaplan, D. J. Richard, P. Nowak, D. J. Malwitz, N. Brooijmans, J. Bard, K. Svenson, J. Lucas, L. Toral-Barza, W. G. Zhang, I. Hollander, J. J. Gibbons, R. T. Abraham, S. Ayral-Kaloustian, T. S. Mansour, K. Yu, J. Med. Chem. 52 (2009) 5013-5016.

[15] A. Zask, J. Kaplan, K. Curran, J.C. Verheijen, D. J. Richard, N. Brooijmans, E. Bennett, J. Lucas, L. Toral-Barza, I. Hollander, J .J. Gibbons, R. T. Abraham, S. Ayral-Kaloustian, T. S. Mansour, K. Yu, Mol Cancer Ther. 8 (2009) B145.

[16] E. Strocchi, F. Fornari, M. Minguzzi, L. Gramantieri, M. Milazzo, V. Rebuttini, S. Breviglieri, C.M. Camaggi, E. Locatelli, L. Bolondi, M. Comes-Franchini, Eur. J. Med. Chem. 48 (2012) 391-401.

[17] H. Kumar, D. Saini, S. Jain, N. Jain, Eur. J. Med. Chem. 70 (2013) 248-258.

[18] A. Balbi, M. Anzaldi, C. Maccio, C. Aiello, M. Mazzei, R. Gangemi, P. Castagnola, M. Miele, C. Rosano, M. Viale, Eur. J. Med. Chem. 46 (2011) 5293-5309.

[19] L. Yuan, C. Song, C. Li, Y. Li, L. Dong, S. Yin, Eur. J. Med. Chem. 67 (2013) 152-157.

[20] J. Sun, X.H. Lv, H.Y. Qiu, Y.T. Wang, Q.R. Du, D.D. Li, Y.H. Yang, H. L. Zhu, Eur. J. Med. Chem. 68 (2013) 1-9.

[21] X. H. Liu, B. F. Ruan, J. X. Liu, B. A. Song, L. H. Jing, J. Li, Y. Yang, H. L. Zhu, X. B. Qi, Bioorg. Med. Chem. Lett. 21 (2011) 2916-2920.

[22] X. H. Liu, H. F. Liu, J. Chen, Y. Yang, B. A. Song, L. S. Bai, J. X. Liu, H. L. Zhu, X. B. Qi, Bioorg. Med. Chem. Lett. 20 (2010) 5705-5708.

[23] W. J. Tang, Y. A. Yang, X. He, J. B. Shi, X. H. Liu, Sci. Rep. 4 (2014), 7106.

[24] G. M. Sheldrick, SHELXTL-97, Program for Crystal Structure Solution and Refinement; University of Göttingen: Göttingen, Germany, 1997.

Figure Captions

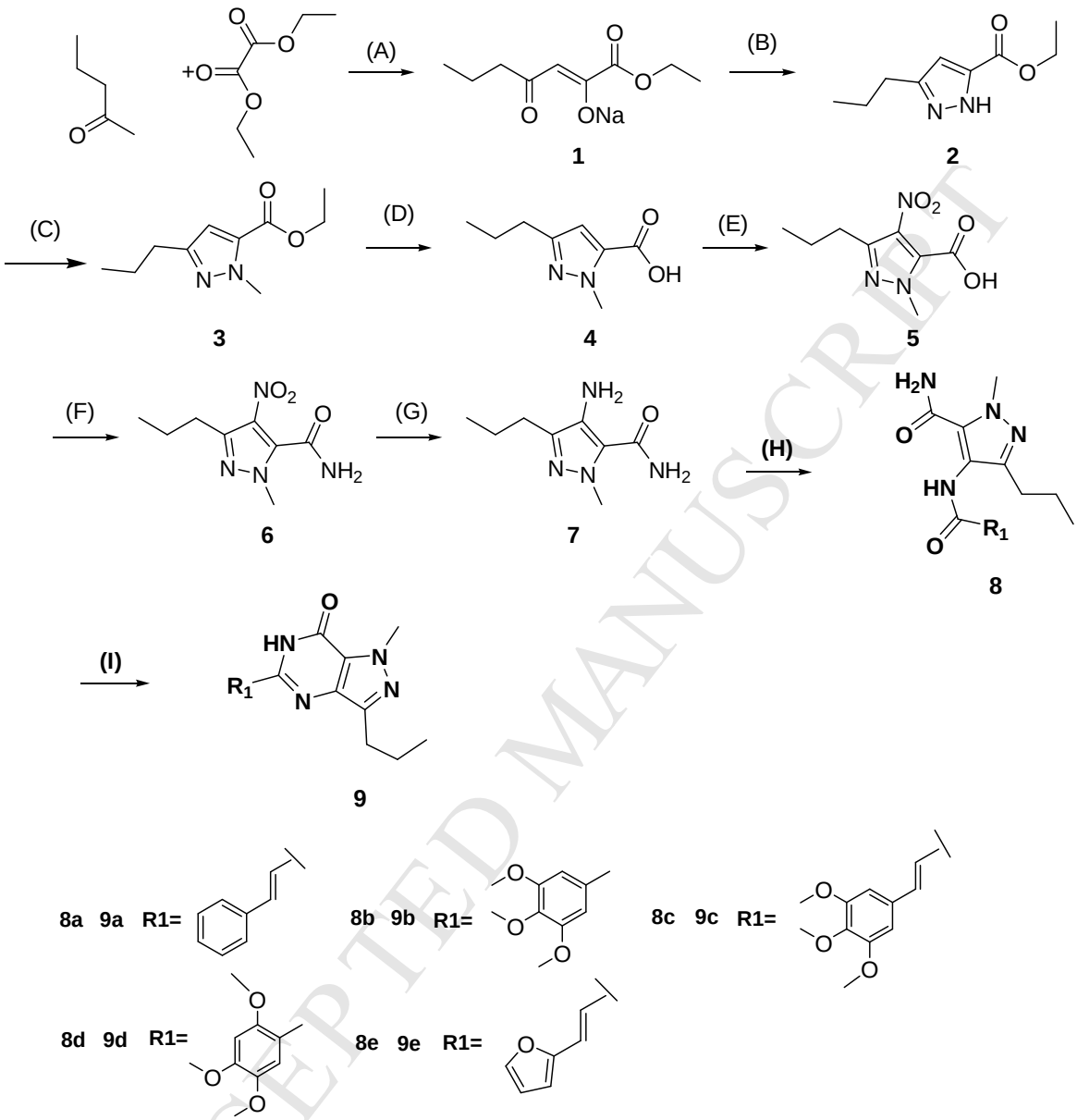

Scheme 1. Synthesis of title compounds **7~9**

Reagent and conditions: (A) Na, EtOH, reflux, 6~8 h; **(B)** NH_2-NH_2•H_2O, 60-65 ^oC, 2 h; **(C)** Dimethyl sulfate, 80 ^oC, 2 h; **(D)** 6 N NaOH, 80 ^oC, 2 h; **(E)** HNO_3/H_2SO_4, 60 ^oC, 4 h; **(F)** a: $SOCl_2$, $CHCl_3$, DMF, reflux, 3 h; b: NH_3•H_2O, 0 ^oC ; **(G)** Tin(II) dichloride dihydrate, EtOH, reflux, 2 h. **(H)** a: Substituted carboxylic acid, $(COCl)_2$, CH_2Cl_2, DMF (Cat), 25 ^oC, 3 h; b: CH_2Cl_2, TEA, 25 ^oC, 12 h; **(I)** NaOEt, EtOH, reflux, 12 h.

Table 1. Cytotoxic activity of the synthesized compounds against SGC-7901, MGC-803, Bcap-37 cell lines [a]

Compound	IC_{50} (μM) [b]		
	SGC-7901	MGC-803	Bcap-37
8a	8.11±0.40	3.44±0.28	46.70±1.77
8b	13.40±1.18	4.57±0.88	40.37±1.98
8c	12.77±1.25	4.24±1.22	55.70±2.21
8d	34.84±1.99	29.51±1.87	33.54±2.01
8e	8.30±1.07	3.01±0.23	10.50±0.87
9a	17.25±1.51	22.60±1.85	45.29±2.98
9b	—	—	—
9c	25.67±1.08	32.75±1.54	37.39±1.69
9d	—	—	—
9e	10.31±0.77	7.14±0.28	28.66±0.95
5-Fluorouracil [c]	6.56±0.39	3.71±0.22	5.18±0.43

[a] The data represented the mean of three experiments in triplicate and were expressed as means ±SD; Only descriptive statistics were done in the text.

[b] The IC_{50} value was defined as the concentration at which 50% survival of cells was observed.

[c] Used as a positive control.

Negative control 0.1%DMSO, no activity.

Table 2. Inhibitory effects of slected compounds against telomerase

Compound	IC_{50} (μM) telomerase [a]
8a	1.98±0.21
8b	7.87±0.69
8c	3.49±0.55
8d	12.20±0.98
8e	1.02±0.08
9c	18.99±1.44
9e	15.17±1.80
Ethidium bromide [b]	2.10±0.11
BIBR1532 [b]	0.28±0.09

[a] Telomerase supercoiling activity

[b] Ethidium bromide and BIBR1532 are reported as a control. The inhibition constant of ethidium toward telomerase has been reported previously.

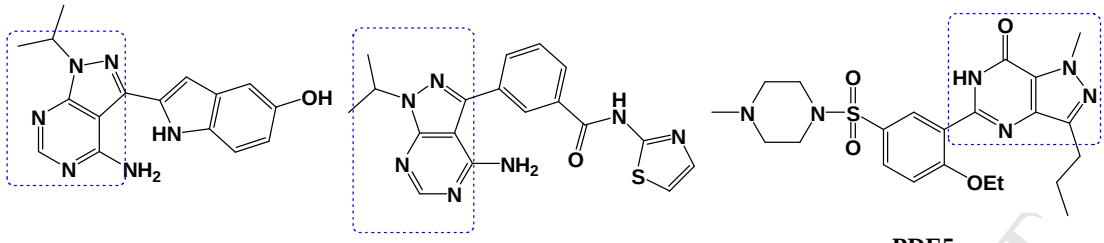

1 **2** **3**

Figure 1. Pyrazole-pyrimidine scaffold based potential candidates and drugs

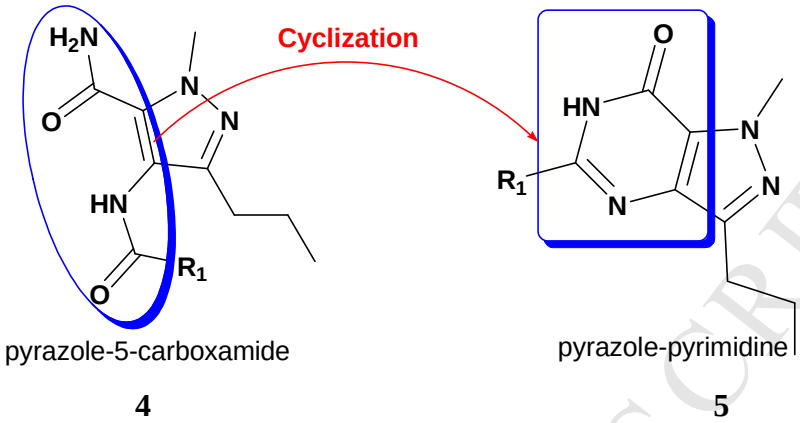

4 **5**

Figure 2. Design of pyrazole-pyrimidine and its precursor scaffold

Figure 3A. ORTEP drawing of compound **8d**

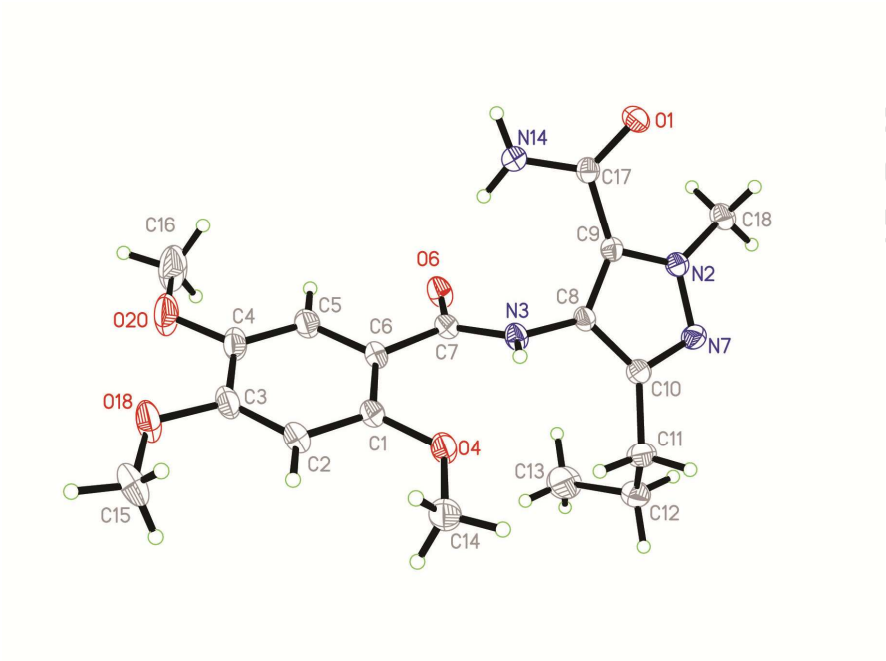

8d

Figure 3B. ORTEP drawing of compound **9a**

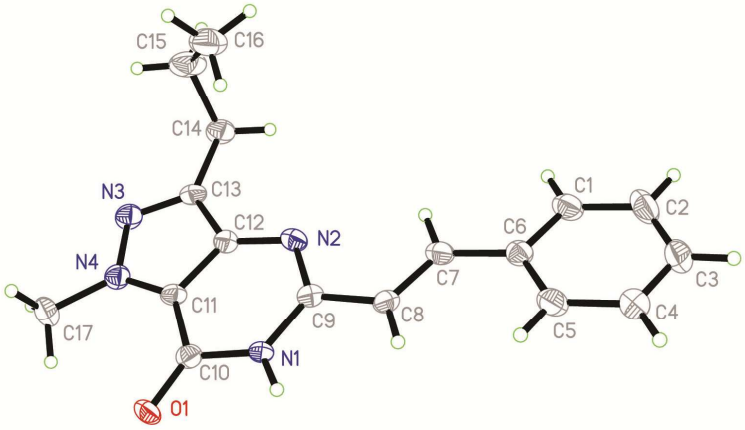

9a

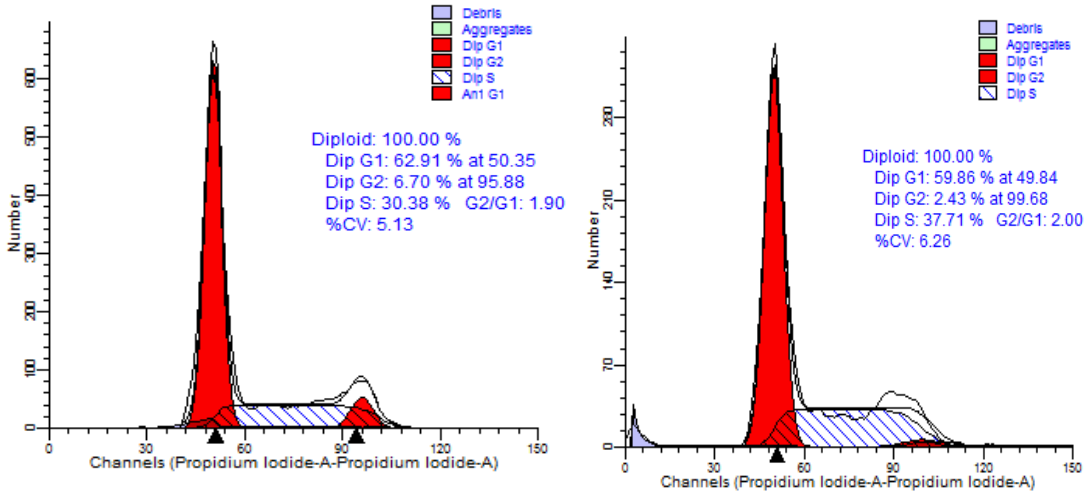

N **8e**

Figure 4. Cells cycle analysis by flow cytometry with MGC-803 cells. MGC-803 cells were incubated with PI and examined by flow cytometry. N, normal; compound **8e** (3 μM), n = 3. Results are the mean ± SD from three independent experiments. * $p<0.05$, ** $p<0.01$ vs control.

Figure 5A. The binding mode between the active conformation of compound **8e** and the protein TERT (PDB code: 3DU6). Panel is a view into the active site cavity

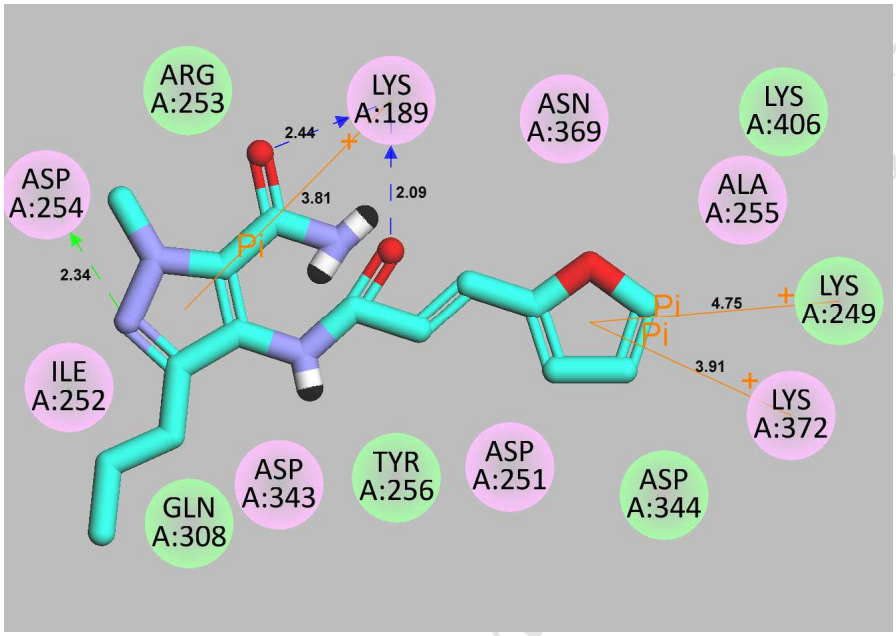

(A). The 2D picture of binding was depicted

Figure 5B. The binding mode between the active conformation of compound **8e** and the protein TERT (PDB code: 3DU6). Panel is a view into the active site cavity

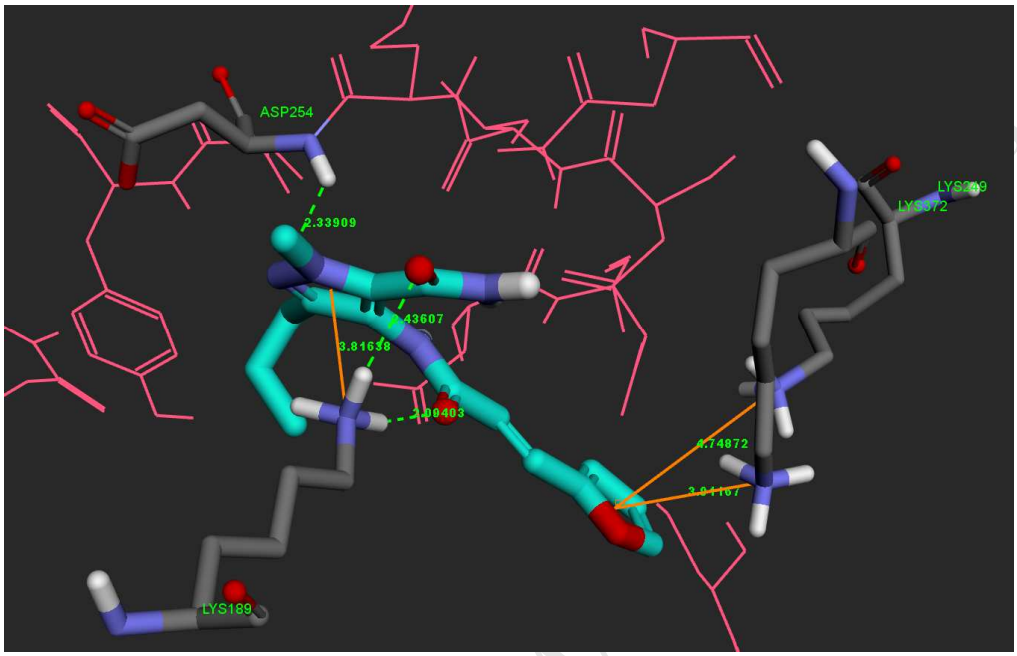

(B). The 3D picture of binding was depicted

Figure 5C. The binding mode between the active conformation of compound **8e** and the protein TERT (PDB code: 3DU6). Panel is a view into the active site cavity

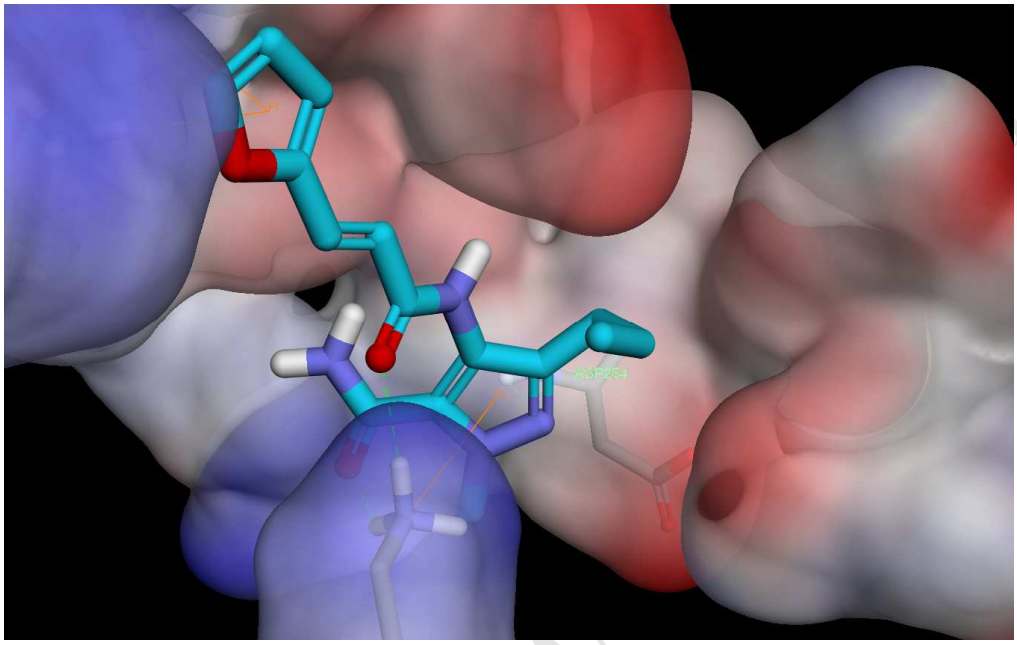

(C). In order to reveal that the molecule was well filled in the active pocket, the enzyme surface was shown

Highlights

► Novel pyrazole-5-carboxamides as potential telomerase inhibitors were designed.

► Compound **8e** exhibited strong inhibitory activity against MGC-803 cells.

►Results also revealed **8e** exhibited the most telomerase inhibitory activity.

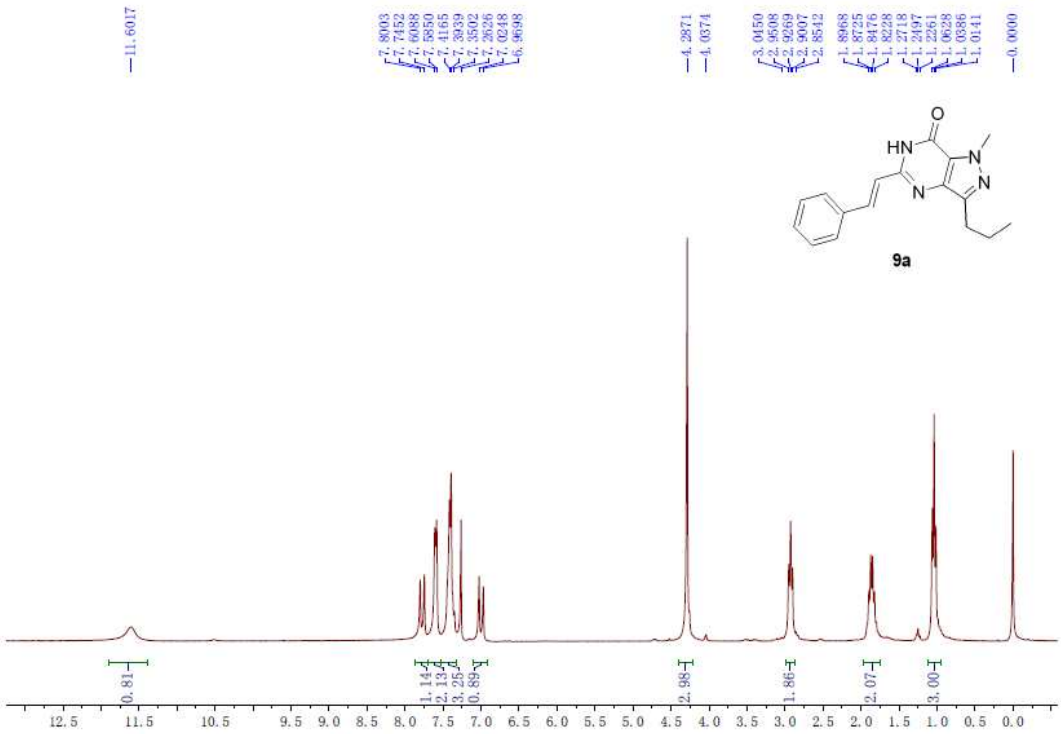
11.6017
7.8003
7.7452
7.6088
7.5850
7.4165
7.3939
7.3502
7.2626
7.0248
6.9698
4.2871
4.0374
3.0450
2.9508
2.9269
2.9007
2.8542
1.8968
1.8725
1.8476
1.8228
1.2718
1.2497
1.2261
1.0628
1.0386
1.0141
0.0000
O
HN
N
N
N
9a
0.81
1.14
2.13
3.25
0.89
2.98
1.86
2.07
3.00

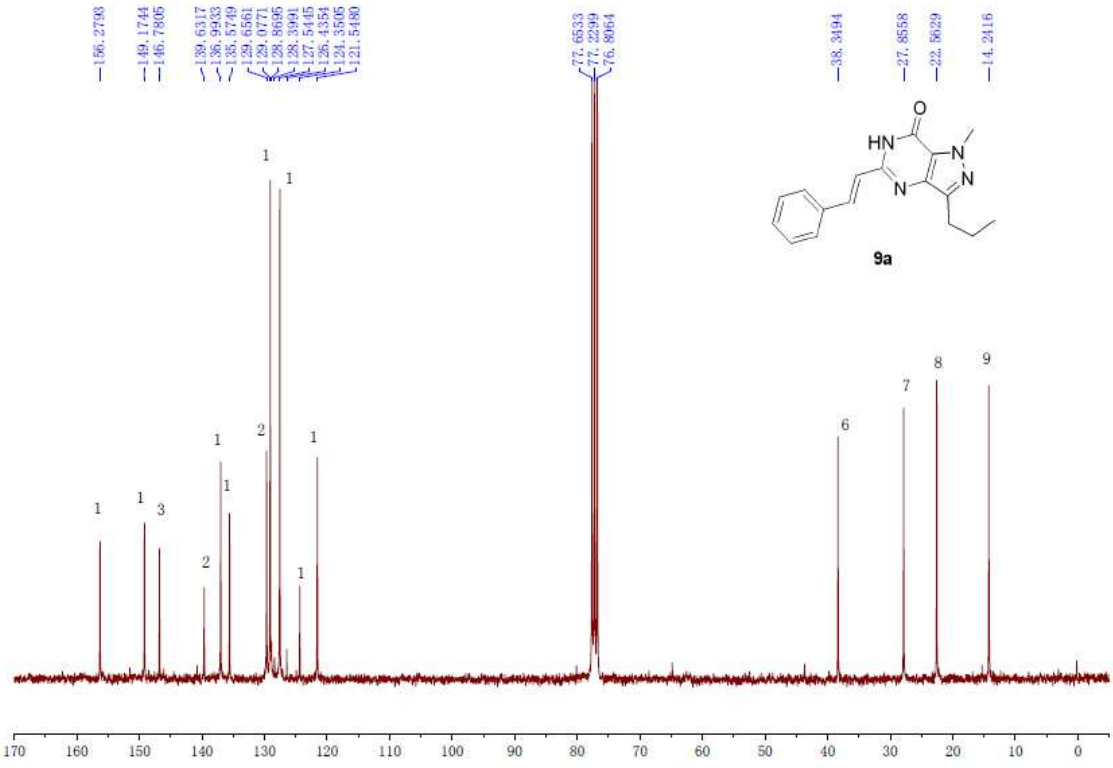
156.2793
149.1744
146.7805
139.6317
136.9933
135.5749
129.6561
129.0771
128.8695
128.3991
127.5445
126.4351
124.3505
121.5480
77.6533
77.2299
76.8064
38.3494
27.8558
22.5629
14.2416
O
HN
N
N
N
9a
1
1
3
2
1
1
2
1
1
1
6
7
8
9

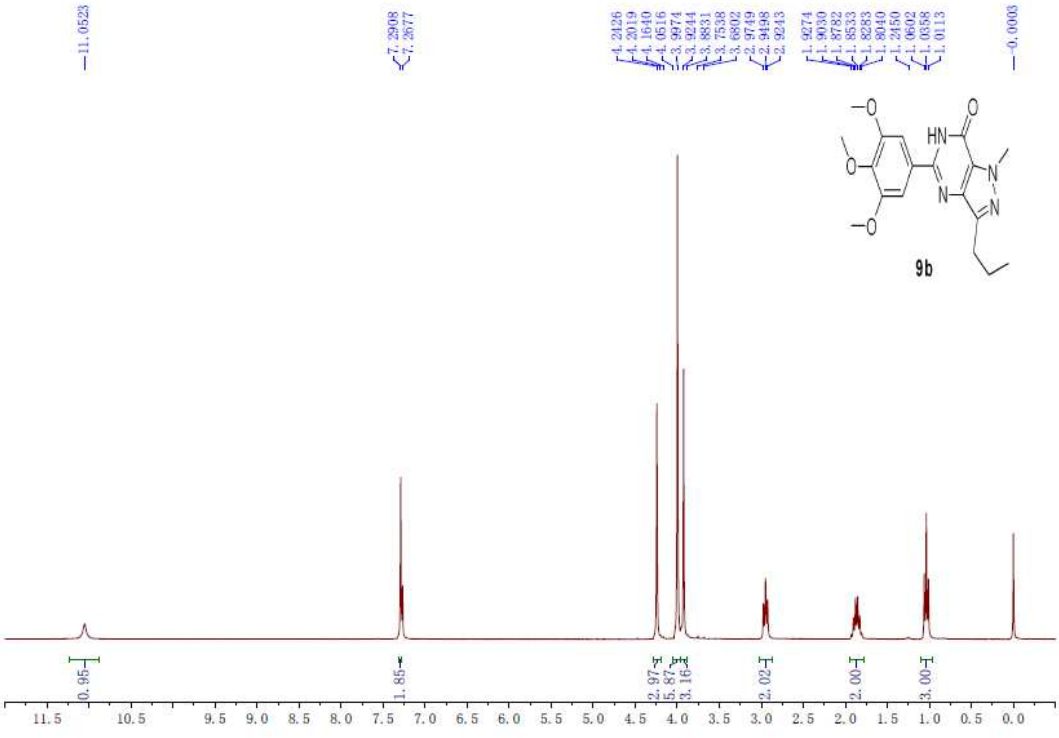
11.0523
7.2908
7.2677
4.2426
4.2019
4.1640
4.0616
3.9474
3.9244
3.8831
3.7538
3.6802
2.9749
2.9498
2.9243
1.9274
1.9030
1.8782
1.8533
1.8283
1.8049
1.2450
1.0602
1.0358
1.0113
-0.0003
HN
O
N
9b
0.95
1.85
2.97
5.87
3.16
2.02
2.00
3.00

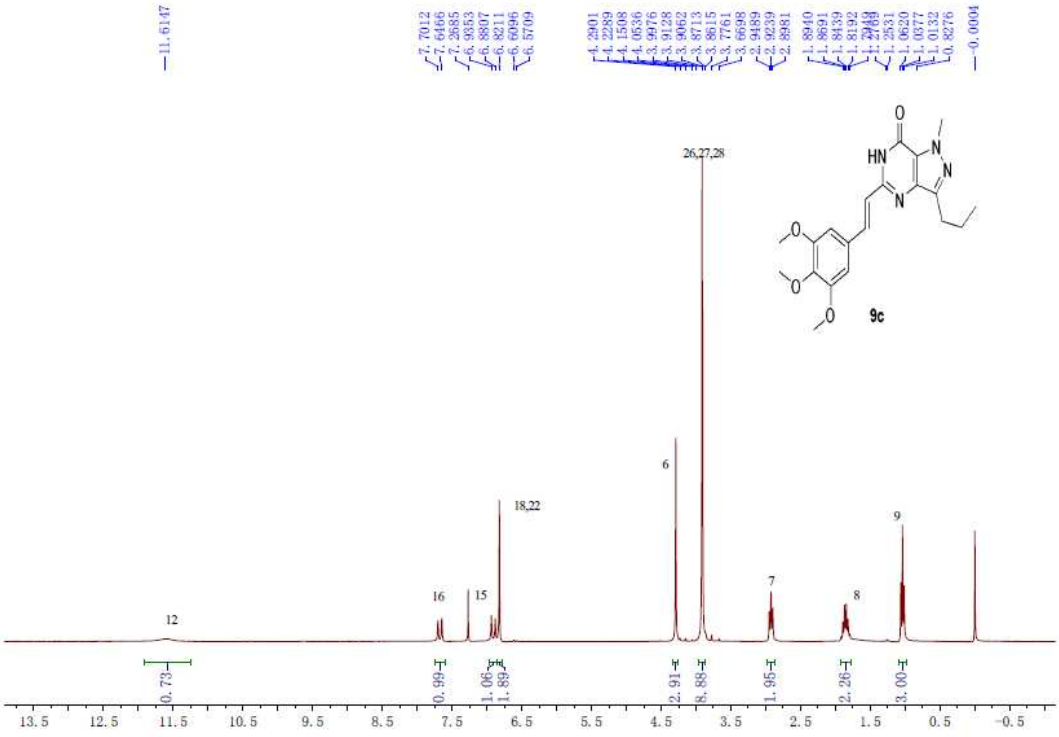
11.6147
7.7012
7.6466
7.3685
6.9353
6.8807
6.8211
6.6096
6.5709
4.2891
4.2289
4.1508
4.0536
3.9476
3.9128
3.9062
3.8713
3.8615
3.7761
3.6698
2.9489
2.9239
2.8981
1.8940
1.8691
1.8439
1.8192
1.2531
1.0620
1.0377
1.0132
0.8276
-0.0004
HN
O
N
9c
26,27,28
6
18,22
9
7
8
16
15
12
0.73
0.99
1.06
1.89
2.91
8.88
1.95
2.26
3.00

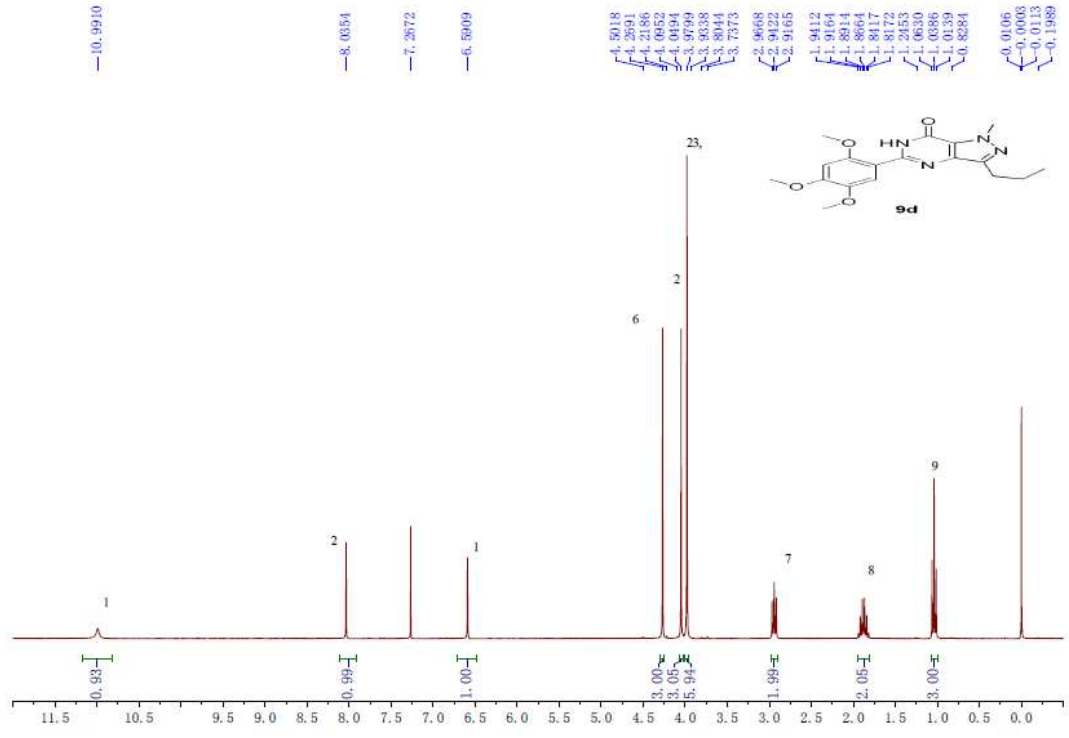
10.9910
8.0354
7.2672
6.5909
4.5018
4.2591
4.2186
4.0952
4.0494
3.9799
3.9338
3.8044
3.7373
2.9668
2.9422
2.9165
1.9412
1.9164
1.8914
1.8664
1.8417
1.8172
1.2453
1.0630
1.0386
1.0139
0.8284
0.0106
-0.0008
-0.0113
-0.1989
9d
0.93
0.99
1.00
3.00
3.05
5.94
1.99
2.05
3.00

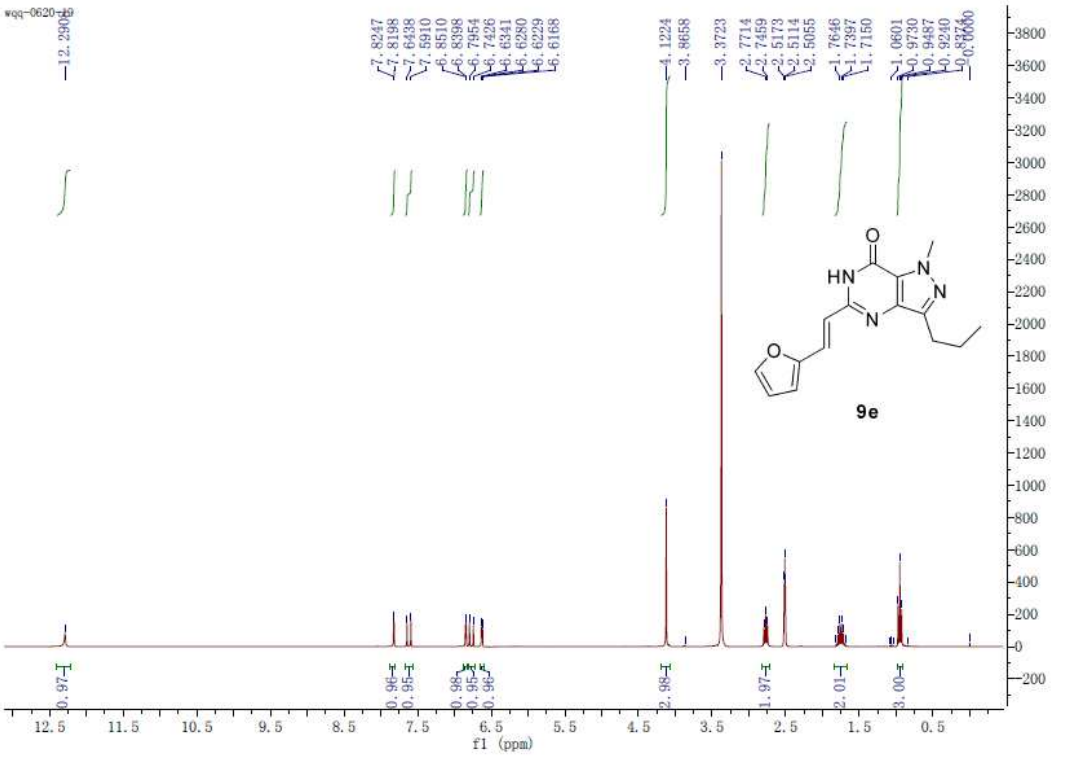
12.2900
7.8247
7.8198
7.6438
7.5910
6.8510
6.8398
6.7954
6.7426
6.6341
6.6280
6.6229
6.6168
4.1224
3.8658
3.3723
2.7714
2.7459
2.5173
2.5114
2.5055
1.7646
1.7397
1.7150
1.0601
0.9730
0.9487
0.9240
0.8374
0.0000
9e
0.97
0.96
0.95
0.99
0.95
0.96
2.98
1.97
2.01
3.00
f1 (ppm)